Acta Cryst C STRUCTURAL CHEMISTRY

ISSN 2053-2296

A new hydrate of magnesium carbonate, $MgCO_3·6H_2O$

Christine Rincke,* Horst Schmidt and Wolfgang Voigt

Institute of Inorganic Chemistry, TU Bergakademie Freiberg, Leipziger Strasse 29, D-09599 Freiberg, Germany.
*Correspondence e-mail: christine.rincke@chemie.tu-freiberg.de

Received 30 October 2019
Accepted 4 February 2020

Edited by V. Langer, Chalmers University of Technology, Sweden

Keywords: magnesium; carbonate; low-temperature hydrate; Raman spectroscopy; crystal structure.

CCDC reference: 1981730

Supporting information: this article has supporting information at journals.iucr.org/c

During investigations of the formation of hydrated magnesium carbonates, a sample of the previously unknown magnesium carbonate hexahydrate ($MgCO_3·6H_2O$) was synthesized in an aqueous solution at 273.15 K. The crystal structure consists of edge-linked isolated pairs of $Mg(CO_3)(H_2O)_4$ octahedra and noncoordinating water molecules, and exhibits similarities to $NiCO_3·5.5H_2O$ (hellyerite). The recorded X-ray diffraction pattern and the Raman spectra confirmed the formation of a new phase and its transformation to magnesium carbonate trihydrate ($MgCO_3·3H_2O$) at room temperature.

1. Introduction

In the $MgO–H_2O–CO_2$ system, besides the thermodynamically stable $MgCO_3$ (magnesite), a variety of hydrated magnesium carbonates are known, which can be divided in basic magnesium carbonates, containing OH^- ions [$Mg_5(CO_3)_4(OH)_2·nH_2O$ and $Mg(CO_3)(OH)_2·nH_2O$], and neutral magnesium carbonates with the composition $MgCO_3·nH_2O$ (Hopkinson *et al.*, 2012; Jauffret *et al.*, 2015). All these phases are of significant relevance in various technological processes, in geological explorations, mineral conversion in the sequestration of CO_2 and in biomineralization (Chaka & Felmy, 2014). Nevertheless, there are many open questions with respect to the conditions of formation, the characterization, the crystal structure and the stability of higher hydrated neutral magnesium carbonates (Hänchen *et al.*, 2008; Hopkinson *et al.*, 2012; Rincke, 2018).

The most frequently investigated neutral magnesium carbonate hydrate, $MgCO_3·3H_2O$ (mineral name: nesquehonite), can be synthesized in the temperature range between 283.15 and 325.15 K (Giester *et al.*, 2000; Frost & Palmer, 2011; Jauffret *et al.*, 2015; Hänchen *et al.*, 2008; Gloss, 1937; Takahashi & Hokoku, 1927; Hopkinson *et al.*, 2012).

At lower temperatures, the pentahydrate, *i.e.* $MgCO_3·5H_2O$ (mineral name: lansfordite), is known. Its crystal structure (monoclinic space group $P2_1/m$) was determined by Liu *et al.* (1990) from a synthetic sample and by Nestola *et al.* (2017) from a mineral. Several possibilities are described to synthesize lansfordite (Ming & Franklin, 1985; Liu *et al.*, 1990). In order to obtain large prismatic crystals, CO_2 can be bubbled through an aqueous suspension of MgO and, subsequently, the crystallization can be carried out in the filtered solution at low temperature (Liu *et al.*, 1990). However, the authors (Liu *et al.*, 1990) did not provide information about the exact CO_2 pressure, the regime of temperature, the concentration of magnesium ions in the solution and the time needed for crystallization. According to Ming & Franklin (1985), these factors are important to avoid the formation of nesquehonite.

Table 1
Experimental details.

Crystal data	
Chemical formula	$MgCO_3·6H_2O$
M_r	192.42
Crystal system, space group	Orthorhombic, *Pbam*
Temperature (K)	200
a, *b*, *c* (Å)	12.3564 (18), 6.5165 (7), 9.9337 (11)
V (Å^3)	799.87 (17)
Z	4
Radiation type	Mo *Kα*
μ (mm^{-1})	0.24
Crystal size (mm)	0.7 × 0.55 × 0.15
Data collection	
Diffractometer	Stoe IPDS 2T
Absorption correction	Integration (Coppens, 1970)
T_{min}, T_{max}	0.694, 0.887
No. of measured, independent and observed [$I > 2\sigma(I)$] reflections	8319, 1143, 965
R_{int}	0.036
(sin $\theta/\lambda)_{max}$ (Å^{-1})	0.687
Refinement	
$R[F^2 > 2\sigma(F^2)]$, $wR(F^2)$, *S*	0.029, 0.085, 1.18
No. of reflections	1143
No. of parameters	83
H-atom treatment	All H-atom parameters refined
$\Delta\rho_{max}$, $\Delta\rho_{min}$ (e Å^{-3})	0.23, −0.26

Computer programs: *X-AREA* (Stoe & Cie, 2015), *X-RED* (Stoe & Cie, 2015), *SHELXS97* (Sheldrick, 2008), *SHELXL2016* (Sheldrick, 2015), *DIAMOND* (Brandenburg, 2017) and *publCIF* (Westrip, 2010).

Furthermore, the solubility of lansfordite is highly dependent on temperature and on CO_2 pressure (Königsberger *et al.*, 1999; Takahashi & Hokoku, 1927; Rincke, 2018). Besides that, there are contradictory statements about the temperature and the rate of conversion of the pentahydrate to the trihydrate. Some research groups have recorded a transition temperature between 283.15 and 288.15 K (Takahashi & Hokoku, 1927; Gloss, 1937; Yanaťeva & Rassonskaya, 1961; Hill *et al.*, 1982; Langmuir, 1965; Ming & Franklin, 1985), while others observed the stability of synthesized and natural samples of lansfordite at room temperature over a period of a few months (Liu *et al.*, 1990; Nestola *et al.*, 2017). Neutral magnesium carbonates with a water content greater than five units per formula are not known up to now. Such highly hydrated neutral carbonates of other bivalent metal ions have been found only for calcium, *i.e.* $CaCO_3·6H_2O$ (ikaite; Hesse *et al.*, 1983), and nickel, *i.e.* $NiCO_3·5.5H_2O$ (hellyerite; Bette *et al.*, 2016). Our own investigations should elucidate the conditions of formation of the magnesium carbonate hydrates.

2. Experimental

2.1. Synthesis and crystallization

To obtain crystals of $MgCO_3·6H_2O$ suitable for single-crystal diffraction analysis (see V11 in Table S1 of the supporting information), carbon dioxide was bubbled through a suspension of magnesium oxide in deionized water (3.1 g, Magnesia M2329, p.a.) for 22 h at 273.15 K. After that, the solution was filtered and stored without stirring at 273.15 K for 16 d until the product crystallized. The product was filtered off for characterization by powder X-ray diffraction and Raman spectroscopy. For intensity data collection, a prismatic crystal of $MgCO_3·6H_2O$ was recovered from a droplet of its mother liquor and mounted rapidly in the cold (200 K) stream of nitrogen gas of the diffractometer.

2.2. Powder X-ray diffraction

The powder X-ray diffraction (PXRD) patterns were taken for phase identification with a Bruker D8 Discover laboratory powder diffractometer in the Bragg–Brentano set-up (Cu $K\alpha_1$ radiation, Vantec 1 detector). The samples were prepared as

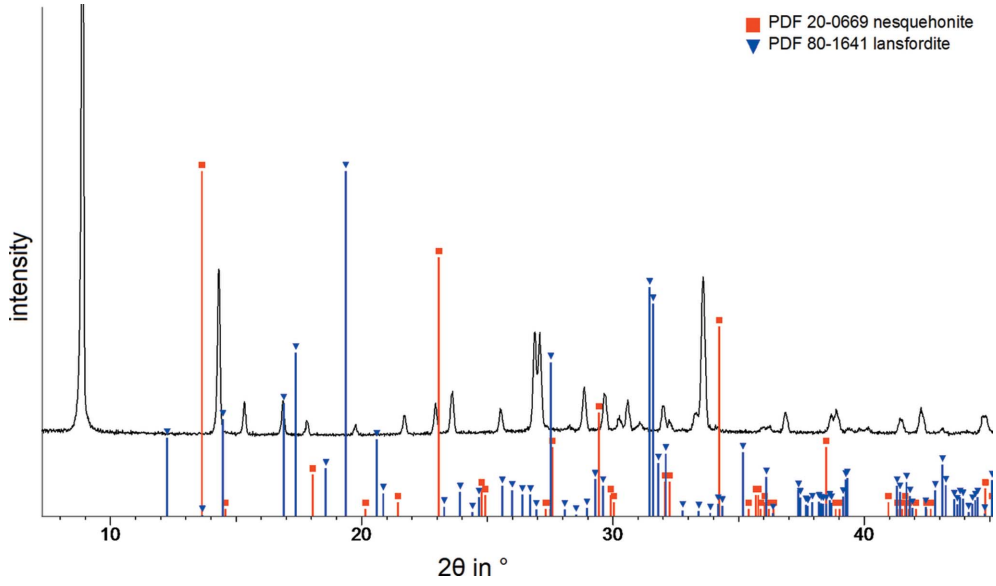

Figure 1
Powder XRD pattern of $MgCO_3·6H_2O$ at low temperature (~273.15 K, Cu *Kα* radiation) and reference data for $MgCO_3·3H_2O$ (PDF 20-0669) and $MgCO_3·5H_2O$ (PDF 80-1641).

Figure 2
Microscopic image of prismatic $MgCO_3{\cdot}6H_2O$ crystals (framed in black) which are partly intergrown. The red-framed crystals are the typical needles of the transformation product $MgCO_3{\cdot}3H_2O$.

flat plates and measured at low temperatures (about 273.15 K) with a home-made cooling box (Rincke, 2018).

2.3. Raman spectroscopy

The Raman spectra were recorded shortly after synthesis with a Bruker RFS100/S FT spectrometer at room temperature (Nd/YAG laser, wavelength of the laser = 1064 nm).

2.4. Refinement

Crystal data, data collection and structure refinement details are given in Table 1. The positions of the H atoms could be located from residual electron-density maxima after further refinement and were refined isotropically.

3. Results and discussion

3.1. Conditions of formation and characterization of magnesium carbonate hexahydrate

On the basis of the information of Liu *et al.* (1990) for the formation of lansfordite, CO_2 was bubbled through aqueous MgO suspensions with various concentrations. After filtration of the solution, the product crystallized at low temperature (273.15–278.15 K), while the CO_2 pressure was decreased by slow degassing of the CO_2 and the solubility product of the carbonate was exceeded. The detailed experimental conditions are given in the supporting information (see Table S1). Characterization of the product with PXRD revealed that nesquehonite is formed at low MgO concentrations, while an unknown phase crystallizes from the solutions at higher Mg^{2+} concentrations, near the solubility of lansfordite at $p(CO_2)$ = 1 bar [$m(Mg^{2+})$ = 0.386 mol $kg^{-1}(H_2O)$ at 273.15 K] (Königsberger *et al.*, 1999; Rincke, 2018). Fig. 1 shows the PXRD pattern of the new product phase in comparison with the reference data for $MgCO_3{\cdot}3H_2O$ and $MgCO_3{\cdot}5H_2O$. The composition of this unknown phase was determined by single-crystal diffraction as $MgCO_3{\cdot}6H_2O$. The pentahydrate was not found in our investigations.

Large prismatic crystals of $MgCO_3{\cdot}6H_2O$ were obtained while using a longer time of crystallization of 16 d (see V11 in Table S1 of the supporting information). These crystals, which are partly intergrown, convert in a few minutes at room temperature into the typical needles of $MgCO_3{\cdot}3H_2O$ (Fig. 2). The process of phase transformation could also be seen by means of Raman spectroscopy (Fig. 3). The assignments of the band positions in comparison with the spectra of nesquehonite and lansfordite are given in the supporting information (Table S2).

Table 2
Selected geometric parameters (Å, °).

Mg1—O1	2.1043 (8)	C1—O4	1.2840 (11)
Mg1—O2	2.0859 (8)	C1—O1	1.2978 (17)
Mg1—O3	2.0672 (8)		
O3—Mg1—O2	86.12 (3)	O1—Mg1—O1^{ii}	81.25 (5)
O2—Mg1—O2^{i}	95.28 (5)	O4—C1—O4^{iii}	120.41 (13)
O3—Mg1—O1	91.46 (4)	O4—C1—O1	119.79 (6)
O2—Mg1—O1	91.74 (3)	Mg1—O1—Mg1^{ii}	98.75 (5)

Symmetry codes: (i) $-x+1, -y, z$; (ii) $-x+1, -y, -z+1$; (iii) $x, y, -z+1$.

3.2. Crystal structure of magnesium carbonate hexahydrate

Magnesium carbonate hexahydrate crystallizes in the orthorhombic space group *Pbam* (No. 55). The Mg1 atom is located on a twofold axis of symmetry. Atoms C1, O1 and O5, and the water molecule H6*A*—O6—H6*B* are positioned on a mirror plane.

Isolated pairs of edge-linked $Mg(CO_3)_2(H_2O)_4$ octahedra are the main building blocks in the crystal structure (Fig. 4).

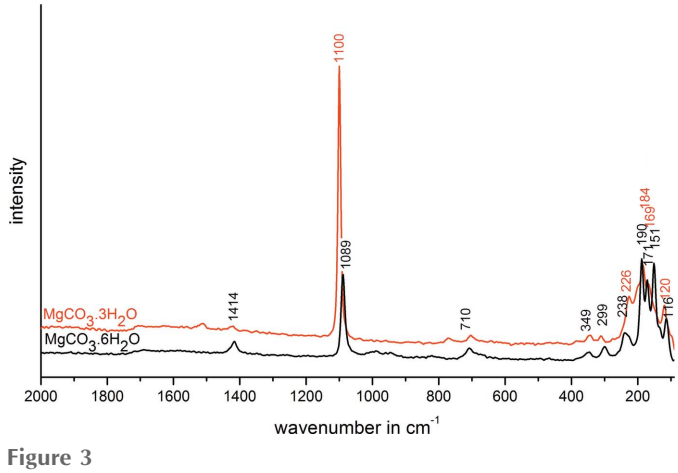

Figure 3
Raman spectrum of $MgCO_3{\cdot}6H_2O$ (black) in comparison with the transformation product $MgCO_3{\cdot}3H_2O$ (red) after storage at room temperature.

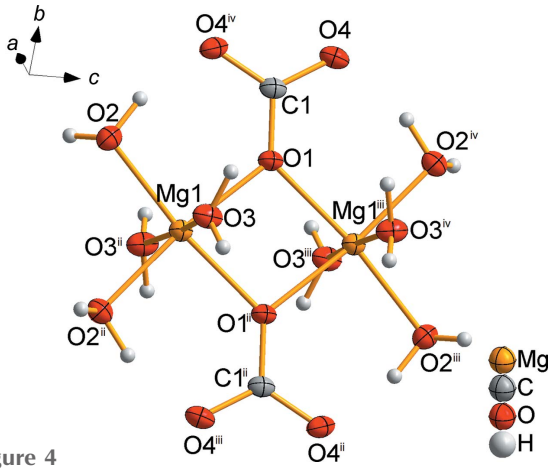

Figure 4
Illustration of the main building block in the crystal structure of $MgCO_3{\cdot}6H_2O$, showing isolated pairs of edge-linked $Mg(CO_3)_2(H_2O)_4$ octahedra [symmetry codes: (ii) $-x+1, -y, z$; (iii) $-x+1, -y, -z+1$; (iv) $x, y, -z+1$].

Table 3
Hydrogen-bond geometry (Å, °).

D—H···A	D—H	H···A	D···A	D—H···A
O5—H5···O2^{iii}	0.812 (18)	2.068 (19)	2.8545 (12)	162.9 (18)
O6—H6B···O5^{ii}	0.87 (3)	1.93 (3)	2.7662 (19)	161 (2)
O6—H6A···O5^{iv}	0.76 (3)	1.99 (3)	2.7137 (19)	160 (3)
O3—H3B···O4^{v}	0.788 (19)	2.025 (19)	2.8055 (12)	170.7 (18)
O3—H3A···O4^{vi}	0.93 (2)	1.77 (2)	2.7001 (12)	174.1 (18)
O2—H2B···O4^{iii}	0.92 (2)	1.70 (2)	2.5868 (12)	162 (2)
O2—H2A···O6	0.84 (2)	1.91 (2)	2.7417 (13)	168.7 (18)

Symmetry codes: (ii) $-x+1, -y, -z+1$; (iii) $x, y, -z+1$; (iv) $x+\frac{1}{2}, -y+\frac{1}{2}, -z+1$; (v) $x-\frac{1}{2}, -y+\frac{1}{2}, -z+1$; (vi) $-x+1, -y+1, -z+1$.

The crystal structure differs significantly from those of $MgCO_3{\cdot}3H_2O$ and $MgCO_3{\cdot}5H_2O$; $MgCO_3{\cdot}3H_2O$ exhibits a monoclinic crystal structure consisting of infinite chains along [010], formed by corner-sharing MgO_6 octahedra and CO_3 groups, which link three MgO_6 octahedra by two common corners and one edge (Giester *et al.*, 2000). In the monoclinic

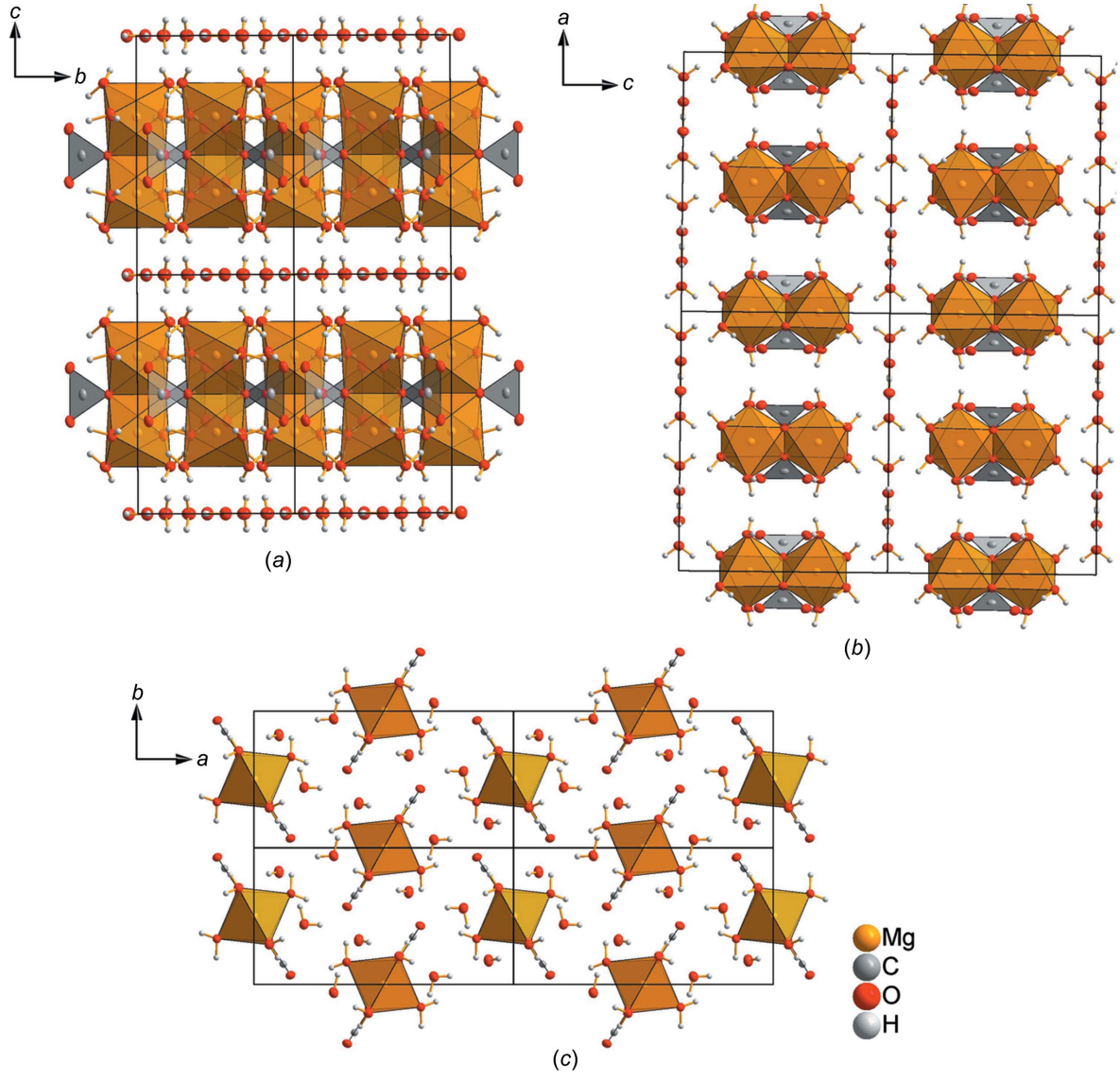

Figure 5
Projection of the crystal structure of $MgCO_3{\cdot}6H_2O$ (*a*) in the *a* direction, (*b*) in the *b* direction and (*c*) in the *c* direction.

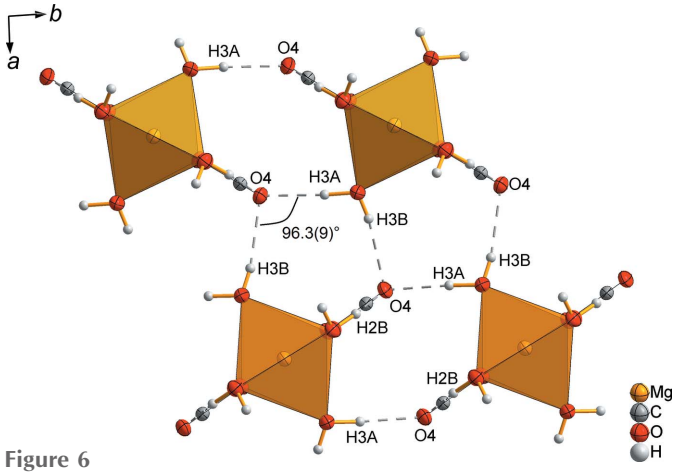

Figure 6
Part of the crystal structure of $MgCO_3{\cdot}6H_2O$, showing the intralayer hydrogen bonds (dashed lines).

crystal structure of $MgCO_3{\cdot}5H_2O$, the characteristic building units are isolated octahedra of $[Mg(CO_3)_2(H_2O)_4]^{2-}$ and $[Mg(H_2O)_6]^{2+}$ (Liu *et al.*, 1990).

The MgO octahedra in $MgCO_3{\cdot}6H_2O$ are slightly distorted (Table 2).

The carbonate units are linked in a monodentate manner to two magnesium ions across the O1 atom. They are planar and exhibit C_{2v} symmetry, because the C1—O1 bond is a little longer than the C1—O4 bond. Furthermore, the O1—C1—O4 angle is a little narrower than the O4—C1—O4^{iv} angle (see Table 2 for numerical data and symmetry code).

The main building blocks are arranged in a sheet-like pattern, perpendicular to the *c* axis (Figs. 5*a* and 5*b*). Within a sheet, every second main building unit is shifted along the $[\frac{1}{2}, \frac{1}{2}, 0]$ direction and rotated by 90°. Consequently, a zigzag-like stacking order results (Fig. 5*c*). The main building units in a sheet are linked by hydrogen bridging bonds (Fig. 6 and Table 3). The sheets are separated by layers of noncoordinating water molecules in the (001) plane.

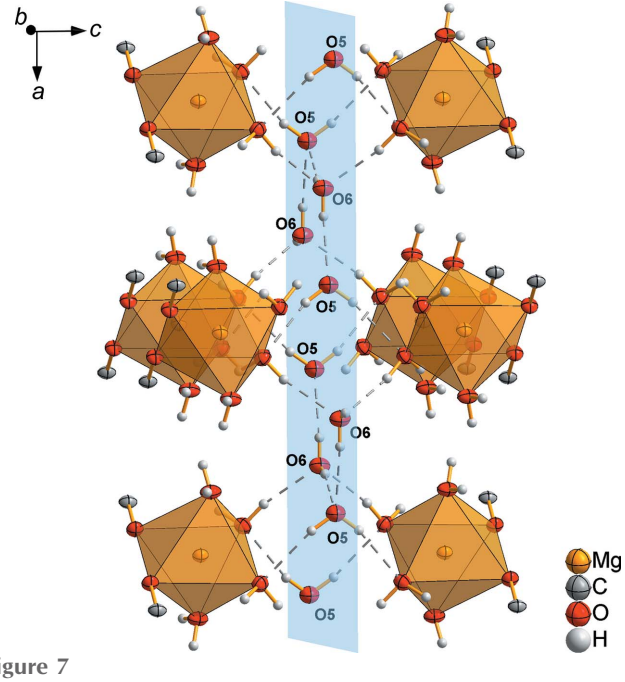

Figure 7
Part of the crystal structure of $MgCO_3{\cdot}6H_2O$, showing the interlayer hydrogen bonds (dashed lines). The (001) plane is shown in blue.

All the atoms of the noncoordinating H6*A*—O6—H6*B* molecule are located in the (001) plane, whereas in the H5—O5—H5^{i} molecule, only the O5 atom is situated in this plane (Fig. 7). The (001) plane is also the mirror plane of this molecule. The noncoordinating water molecules are linked by hydrogen bridging bonds both in the (001) plane among themselves and with the MgO octahedra. Thus, the crystal structure is three-dimensional crosslinked (Fig. 7).

3.3. Comparison with crystal structures of other carbonate hydrates of bivalent metal ions

Other neutral carbonate hydrates of bivalent metal ions with a water content greater than five units per formula are only known for calcium ($CaCO_3{\cdot}6H_2O$) and nickel ($NiCO_3{\cdot}5.5H_2O$). Like the title compound, these phases can be synthesized only at low temperatures of about 273.15 K and are transformed at room temperature to $CaCO_3$ (Coleyshaw *et al.*, 2003) and amorphous nickel carbonate (Bette *et al.*, 2016; Rincke, 2018), respectively.

The crystal structure of $CaCO_3{\cdot}6H_2O$ is significantly different from that of $MgCO_3{\cdot}6H_2O$ for the very reason that the coordination number of the cation in $CaCO_3{\cdot}6H_2O$ is eight and not six as in $MgCO_3{\cdot}6H_2O$ (Dickens & Brown, 1970; Hesse *et al.*, 1983).

However, the radii of nickel and magnesium ions are very similar and actually the crystal structures of $NiCO_3{\cdot}5.5H_2O$ and $MgCO_3{\cdot}6H_2O$ exhibit similarities. Both crystal structures consist of isolated edge-linked pairs of $M(CO_3)(H_2O)_4$ (*M* = Mg or Ni), which are the main building units and are arranged in sheets, together with noncoordinating water molecules, perpendicular to the *c* axis. The symmetry of $NiCO_3{\cdot}5.5H_2O$ is lower; it crystallizes in the monoclinic group *P*2/*n*. As a consequence, there are two crystallographically different Ni atoms. In contrast to $MgCO_3{\cdot}6H_2O$, in $NiCO_3{\cdot}5.5H_2O$, the NiO octahedra of Ni2 are not rotated by 90° (Bette *et al.*, 2016).

4. Conclusion

A new neutral magnesium carbonate with the previously unknown high water content of six units per formula, *i.e.* $MgCO_3{\cdot}6H_2O$, was produced by passing gaseous CO_2 through an aqueous suspension of MgO and storing the filtered solution at 273.15 K. The X-ray diffraction pattern and Raman spectra confirmed the formation of the new phase and its transformation to $MgCO_3{\cdot}3H_2O$. $MgCO_3{\cdot}5H_2O$ was not found in our study. Obviously, the formation conditions of magnesium carbonate hydrates depend on the concentration of the MgO suspension, the CO_2 pressure, the temperature regime and the time of storage. Therefore, it would be useful to carry out further systematic investigations on the chemical kinetics of the formation of the magnesium carbonate hydrates.

The crystal structure of $MgCO_3{\cdot}6H_2O$ differs significantly from the other known magnesium carbonate hydrates, because the main building units are isolated pairs of edge-linked $Mg(CO_3)(H_2O)_4$ octahedra and free water molecules in the (001) plane, but it exhibits similarities to the nickel salt, $NiCO_3{\cdot}5.5H_2O$ (hellyerite).

References

Bette, S., Rincke, C., Dinnebier, R. E. & Voigt, W. (2016). *Z. Anorg. Allg. Chem.* **642**, 652–659.

Brandenburg, K. (2017). *DIAMOND*. Crystal Impact GbR, Bonn, Germany.

Chaka, A. M. & Felmy, A. R. (2014). *J. Phys. Chem. A*, **118**, 7469–7488.

Coleyshaw, E. E., Crump, G. & Griffith, W. P. (2003). *Spectrochim. Acta A Mol. Biomol. Spectrosc.* **59**, 2231–2239.

Coppens, P. (1970). *Crystallographic Computing*, edited by F. R. Ahmed, S. R. Hall & C. P. Huber, pp. 255–270. Copenhagen: Munksgaard.

Dickens, B. & Brown, W. E. (1970). *Inorg. Chem.* **9**, 480–486.

Frost, R. L. & Palmer, S. J. (2011). *Spectrochim. Acta A Mol. Biomol. Spectrosc.* **78**, 1255–1260.

Giester, G., Lengauer, C. L. & Rieck, B. (2000). *Mineral. Petrol.* **70**, 153–163.

Gloss, G. (1937). Dissertation. Friedrich-Wilhelms-University of Berlin, Germany.

Hänchen, M., Prigiobbe, V., Baciocchi, R. & Mazzotti, M. (2008). *Chem. Eng. Sci.* **63**, 1012–1028.

Hesse, K. F., Kueppers, H. & Suess, E. (1983). *Z. Kristallogr.* **163**, 227–231.

Hill, R. J., Canterford, J. H. & Moyle, F. J. (1982). *Miner. Mag.* **46**, 453–457.

Hopkinson, L., Kristova, P., Rutt, K. & Cressey, G. (2012). *Geochim. Cosmochim. Acta*, **76**, 1–13.

Jauffret, G., Morrison, J. & Glasser, F. P. (2015). *J. Therm. Anal. Calorim.* **122**, 601–609.

Königsberger, E., Königsberger, L.-C. & Gamsjäger, H. (1999). *Geochim. Cosmochim. Acta*, **63**, 3105–3119.

Langmuir, D. (1965). *J. Geol.* **73**, 730–754.

Liu, B., Zhou, X., Cui, X. & Tang, J. (1990). *Sci. China Ser. B*, **33**, 1350–1356.

Ming, D. W. & Franklin, W. T. (1985). *Soil Sci. Soc. Am. J.* **49**, 1303–1308.

Nestola, F., Kasatkin, A. V., Potapov, S. S., Chervyatsova, O. Y. & Lanza, A. (2017). *Miner. Mag.* **81**, 1063–1071.

Rincke, C. (2018). Dissertation, TU Bergakademie Freiberg. Freiberg, Germany.

Sheldrick, G. M. (2008). *Acta Cryst.* A**64**, 112–122.

Sheldrick, G. M. (2015). *Acta Cryst.* C**71**, 3–8.

Stoe & Cie (2015). *X-AREA* and *X-RED*. Stoe & Cie, Darmstadt, Germany.

Takahashi, G. & Hokoku, E. S. (1927). *Bull. Imp. Hyg. Lab.* **29**, 165–251.

Westrip, S. P. (2010). *J. Appl. Cryst.* **43**, 920–925.

Yanaťeva, O. K. & Rassonskaya, I. S. (1961). *Zh. Neorg. Khim.* **6**, 1424–1430.

supporting information

Acta Cryst. (2020). C**76**, 244-249 [https://doi.org/10.1107/S2053229620001540]

A new hydrate of magnesium carbonate, $MgCO_3·6H_2O$

Christine Rincke, Horst Schmidt and Wolfgang Voigt

Computing details

Data collection: *X-AREA* (Stoe & Cie, 2015); cell refinement: *X-AREA* (Stoe & Cie, 2015); data reduction: *X-RED* (Stoe & Cie, 2015); program(s) used to solve structure: *SHELXS97* (Sheldrick, 2008); program(s) used to refine structure: *SHELXL2016* (Sheldrick, 2015); molecular graphics: *DIAMOND* (Brandenburg, 2017); software used to prepare material for publication: *publCIF* (Westrip, 2010).

Magnesium carbonate hexahysrate

Crystal data

$MgCO_3·6H_2O$
M_r = 192.42
Orthorhombic, *Pbam*
a = 12.3564 (18) Å
b = 6.5165 (7) Å
c = 9.9337 (11) Å
V = 799.87 (17) Å^3
Z = 4
F(000) = 408
D_x = 1.598 Mg m^{-3}
Mo *Kα* radiation, *λ* = 0.71073 Å
Cell parameters from 9707 reflections
θ = 2.7–27.0°
μ = 0.24 mm^{-1}
T = 200 K
Prism, colorless
0.7 × 0.55 × 0.15 mm

Data collection

Stoe IPDS 2T diffractometer
Radiation source: sealed X-ray tube, 12 x 0.4 mm long-fine focus
Plane graphite monochromator
Detector resolution: 6.67 pixels mm^{-1}
rotation method scans
Absorption correction: integration (Coppens, 1970)
T_{min} = 0.694, T_{max} = 0.887
8319 measured reflections
1143 independent reflections
965 reflections with $I > 2\sigma(I)$
R_{int} = 0.036
θ_{max} = 29.2°, θ_{min} = 3.3°
h = −16→16
k = −7→8
l = −13→11

Refinement

Refinement on F^2
Least-squares matrix: full
$R[F^2 > 2\sigma(F^2)]$ = 0.029
$wR(F^2)$ = 0.085
S = 1.18
1143 reflections
83 parameters
0 restraints
Primary atom site location: structure-invariant direct methods
Hydrogen site location: difference Fourier map
All H-atom parameters refined
$w = 1/[\sigma^2(F_o^2) + (0.0483P)^2 + 0.1805P]$ where $P = (F_o^2 + 2F_c^2)/3$
$(\Delta/\sigma)_{max} < 0.001$
$\Delta\rho_{max}$ = 0.23 e Å^{-3}
$\Delta\rho_{min}$ = −0.26 e Å^{-3}

Special details

Geometry. All esds (except the esd in the dihedral angle between two l.s. planes) are estimated using the full covariance matrix. The cell esds are taken into account individually in the estimation of esds in distances, angles and torsion angles; correlations between esds in cell parameters are only used when they are defined by crystal symmetry. An approximate (isotropic) treatment of cell esds is used for estimating esds involving l.s. planes.

Fractional atomic coordinates and isotropic or equivalent isotropic displacement parameters (Å²)

	x	*y*	*z*	U_{iso}*/U_{eq}
Mg1	0.500000	0.000000	0.33923 (5)	0.01691 (15)
C1	0.61245 (11)	0.3494 (2)	0.500000	0.0176 (3)
O1	0.55574 (8)	0.18176 (16)	0.500000	0.0189 (2)
O2	0.55982 (7)	0.20756 (12)	0.19775 (8)	0.02241 (19)
O3	0.35722 (6)	0.16456 (13)	0.32879 (9)	0.0230 (2)
O4	0.64098 (6)	0.43100 (12)	0.61217 (8)	0.0228 (2)
O5	0.40386 (10)	0.3240 (2)	1.000000	0.0294 (3)
O6	0.69316 (10)	0.0585 (2)	0.000000	0.0277 (3)
H2A	0.6079 (17)	0.167 (3)	0.1436 (18)	0.039 (5)*
H2B	0.5913 (18)	0.305 (3)	0.252 (3)	0.057 (6)*
H3A	0.3553 (17)	0.302 (3)	0.3545 (18)	0.043 (5)*
H3B	0.2986 (16)	0.124 (3)	0.3454 (16)	0.033 (4)*
H6A	0.755 (2)	0.062 (4)	0.000000	0.039 (7)*
H6B	0.678 (2)	−0.071 (5)	0.000000	0.040 (7)*
H5	0.4421 (17)	0.310 (3)	0.9341 (18)	0.048 (5)*

Atomic displacement parameters (Å²)

	U^{11}	U^{22}	U^{33}	U^{12}	U^{13}	U^{23}
Mg1	0.0166 (2)	0.0156 (3)	0.0185 (2)	−0.00105 (17)	0.000	0.000
C1	0.0141 (6)	0.0140 (6)	0.0246 (6)	0.0010 (5)	0.000	0.000
O1	0.0199 (5)	0.0155 (5)	0.0213 (5)	−0.0044 (4)	0.000	0.000
O2	0.0227 (4)	0.0227 (4)	0.0219 (4)	−0.0016 (3)	0.0023 (3)	0.0024 (3)
O3	0.0174 (4)	0.0188 (4)	0.0328 (4)	0.0004 (3)	0.0011 (3)	−0.0025 (3)
O4	0.0230 (4)	0.0174 (4)	0.0281 (4)	−0.0031 (3)	−0.0031 (3)	−0.0031 (3)
O5	0.0228 (6)	0.0363 (7)	0.0290 (6)	0.0013 (5)	0.000	0.000
O6	0.0220 (6)	0.0280 (6)	0.0331 (6)	−0.0022 (5)	0.000	0.000

Geometric parameters (Å, º)

Mg1—O1	2.1043 (8)	O3—H3A	0.93 (2)
Mg1—O2	2.0859 (8)	O3—H3B	0.788 (19)
Mg1—O3	2.0672 (8)	O5—H5	0.812 (18)
C1—O4	1.2840 (11)	O5—H5^{i}	0.812 (18)
C1—O1	1.2978 (17)	O6—H6A	0.76 (3)
O2—H2A	0.84 (2)	O6—H6B	0.87 (3)
O2—H2B	0.92 (2)		
O3—Mg1—O2	86.12 (3)	O3^{ii}—Mg1—Mg1^{iii}	92.87 (3)

O2—Mg1—O2^{ii}	95.28 (5)	O3—Mg1—Mg1^{iii}	92.87 (3)
O3—Mg1—O1	91.46 (4)	O2^{ii}—Mg1—Mg1^{iii}	132.36 (3)
O2—Mg1—O1	91.74 (3)	O2—Mg1—Mg1^{iii}	132.36 (3)
O1—Mg1—O1^{iii}	81.25 (5)	O1^{iii}—Mg1—Mg1^{iii}	40.63 (2)
O4—C1—O4^{iv}	120.41 (13)	O1—Mg1—Mg1^{iii}	40.63 (2)
O4—C1—O1	119.79 (6)	O4^{iv}—C1—O1	119.79 (6)
Mg1—O1—Mg1^{iii}	98.75 (5)	C1—O1—Mg1^{iii}	130.58 (2)
O3^{ii}—Mg1—O3	174.25 (5)	C1—O1—Mg1	130.58 (2)
O3^{ii}—Mg1—O2^{ii}	86.12 (3)	Mg1—O2—H2A	118.3 (12)
O3—Mg1—O2^{ii}	90.01 (3)	Mg1—O2—H2B	101.9 (14)
O3^{ii}—Mg1—O2	90.01 (3)	H2A—O2—H2B	106.9 (19)
O3^{ii}—Mg1—O1^{iii}	91.46 (4)	Mg1—O3—H3A	120.5 (13)
O3—Mg1—O1^{iii}	92.91 (4)	Mg1—O3—H3B	126.9 (13)
O2^{ii}—Mg1—O1^{iii}	91.74 (3)	H3A—O3—H3B	103.9 (18)
O2—Mg1—O1^{iii}	172.90 (4)	H5—O5—H5^{i}	107 (3)
O3^{ii}—Mg1—O1	92.91 (4)	H6A—O6—H6B	105 (3)
O2^{ii}—Mg1—O1	172.91 (4)		

Symmetry codes: (i) *x*, *y*, −*z*+2; (ii) −*x*+1, −*y*, *z*; (iii) −*x*+1, −*y*, −*z*+1; (iv) *x*, *y*, −*z*+1.

Hydrogen-bond geometry (Å, º)

D—H···*A*	*D*—H	H···*A*	*D*···*A*	*D*—H···*A*
O5—H5···O2^{iv}	0.812 (18)	2.068 (19)	2.8545 (12)	162.9 (18)
O6—H6*B*···O5^{iii}	0.87 (3)	1.93 (3)	2.7662 (19)	161 (2)
O6—H6*A*···O5^{v}	0.76 (3)	1.99 (3)	2.7137 (19)	160 (3)
O3—H3*B*···O4^{vi}	0.788 (19)	2.025 (19)	2.8055 (12)	170.7 (18)
O3—H3*A*···O4^{vii}	0.93 (2)	1.77 (2)	2.7001 (12)	174.1 (18)
O2—H2*B*···O4^{iv}	0.92 (2)	1.70 (2)	2.5868 (12)	162 (2)
O2—H2*A*···O6	0.84 (2)	1.91 (2)	2.7417 (13)	168.7 (18)

Symmetry codes: (iii) −*x*+1, −*y*, −*z*+1; (iv) *x*, *y*, −*z*+1; (v) *x*+1/2, −*y*+1/2, −*z*+1; (vi) *x*−1/2, −*y*+1/2, −*z*+1; (vii) −*x*+1, −*y*+1, −*z*+1.